

Supporting Information

ROS-targeted Depression Therapy *via* BSA-incubated Ceria Nanocluster

Shengyang Fu^{1‡}, *Huili Chen*^{1‡}, *Weitao Yang*^{2, 3, 4}, *Xiaohuan Xia*^{1, 4, 5*}, *Shu Zhao*¹,
*Xiaonan Xu*¹, *Pu Ai*^{1, 6}, *Qingyuan Cai*^{1, 7}, *Xiangyu Li*¹, *Yi Wang*⁸, *Jie Zhu*⁹, *Bingbo Zhang*^{2, 3, 4*}, *Jialin C. Zheng*^{1, 3, 4*}

¹Center for Translational Neurodegeneration and Regenerative Therapy, Tongji Hospital affiliated to Tongji University School of Medicine, Shanghai 200065, China.

²The Institute for Translational Nanomedicine, Shanghai East Hospital, Shanghai 200120, China.

³The Institute for Biomedical Engineering & Nano Science, School of Medicine, Tongji University, Shanghai 200092, China.

⁴Shanghai Frontiers Science Center of Nanocatalytic Medicine, Tongji University School of Medicine, Shanghai 200331, China.

⁵Translational Research Institute of Brain and Brain-Like Intelligence, Shanghai Fourth People's Hospital affiliated to Tongji University School of Medicine, Shanghai 200434, China.

⁶Wuxi Clinical College of Anhui Medical University, Hefei 230022, China.

⁷Franklin & Marshall College, PA, 17603, United States.

⁸Center for Translational Neurodegeneration and Regenerative Therapy, Yangzhi Rehabilitation Hospital affiliated to Tongji University, Shanghai 200065, China.

⁹Center for Translational Neurodegeneration and Regenerative Therapy, Shanghai Tenth People's Hospital affiliated to Tongji University School of Medicine, Shanghai 200065, China.

Contents

Supplemental Figure 1

Supplemental Figure 2

Supplemental Figure 3

Supplemental Figure 4

Supplemental Figure 5

Supplemental Figure 6

Supplemental Figure 7

Supplemental Figure 8

Supplemental Figure 9

Supplemental Figure 10

Supplemental Figure 11

Supplemental Figure 12

Supplemental Figure 13

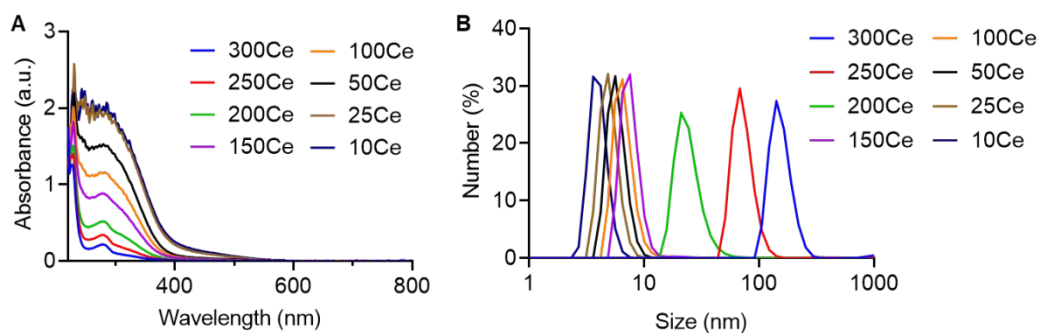
Supplemental Figure 14

Supplemental Table 1

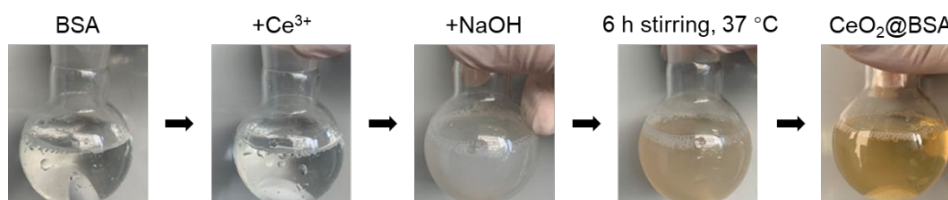
Supplemental Table 2

Supplemental Table 3

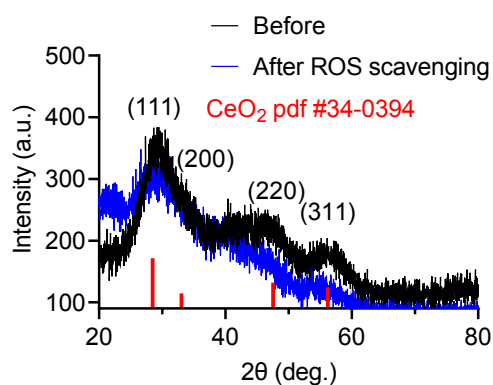
Supplemental Materials and Methods



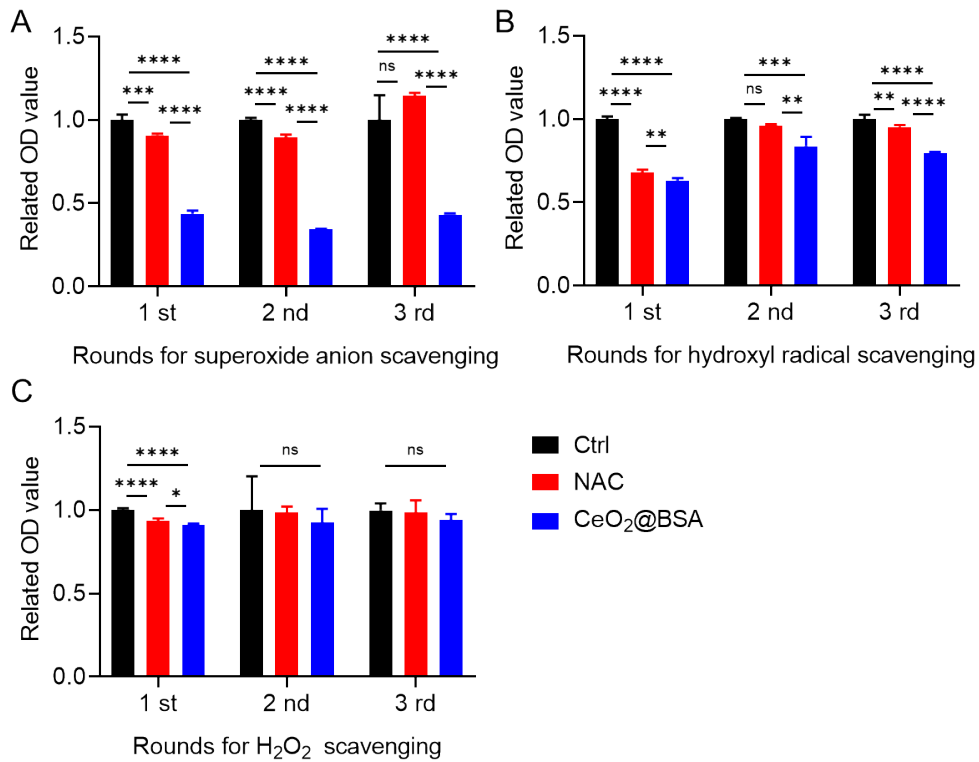
Supplementary Figure 1. (A) Uv-vis and (B) DLS characterization of CeO₂@BSA. (The synthetic ratio of BSA/Ce³⁺ for preparing CeO₂@BSA was listed in Supplementary Table 1)



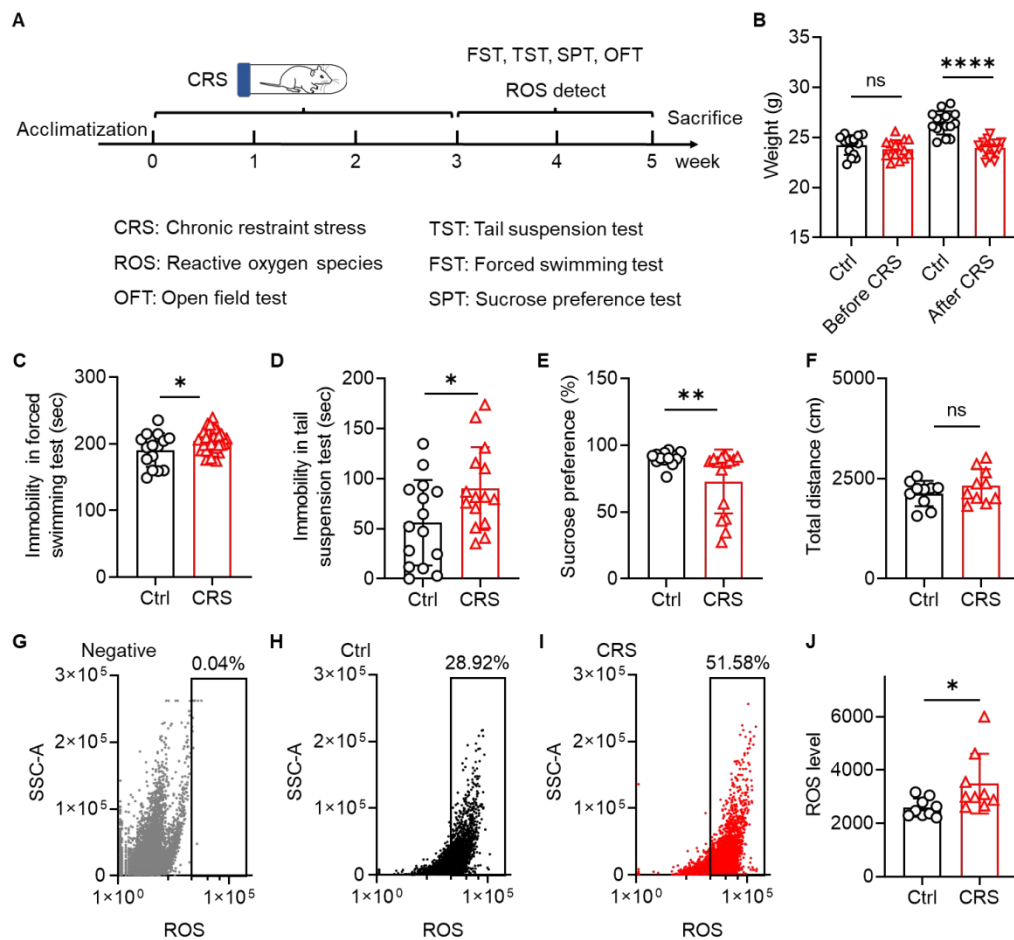
Supplementary Figure 2. CeO₂@BSA nanoclusters synthesis. Ce³⁺ was pre-anchored in BSA, and assembled into nanocluster under an alkali-induced redox environment, and finally obtained a clarified buff solution.



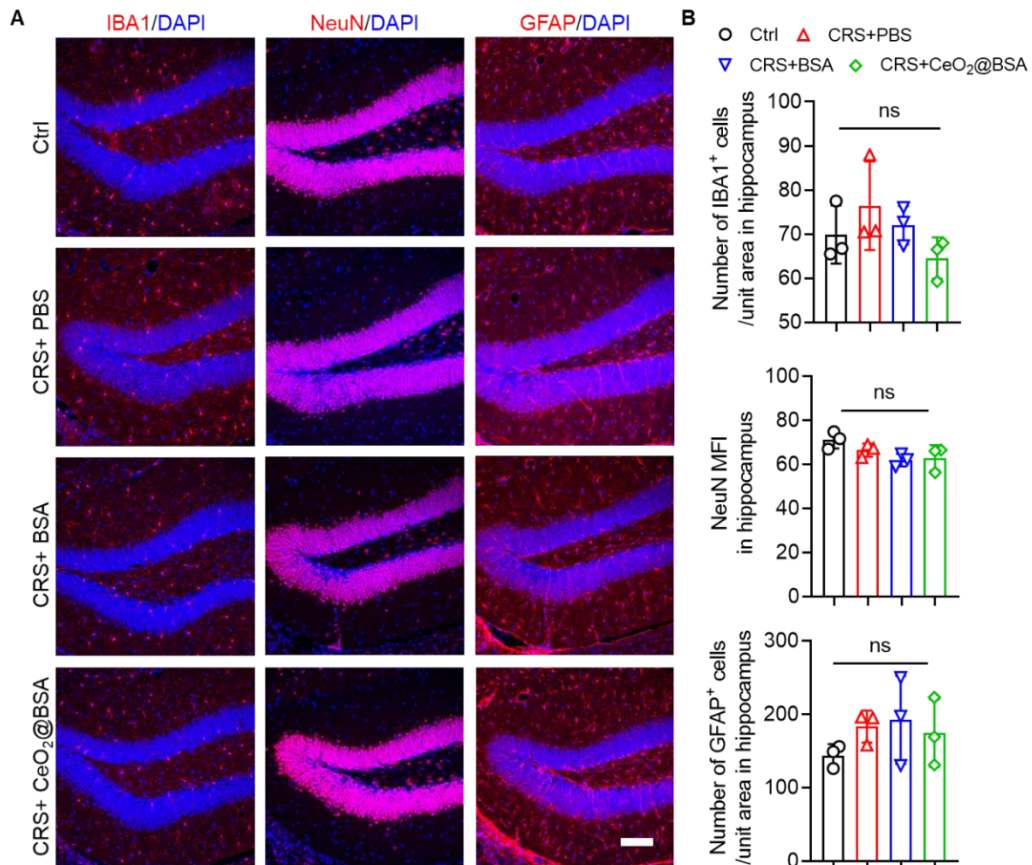
Supplementary Figure 3. The XRD patterns of CeO₂@BSA nanocluster before and after ROS scavenging reactions.



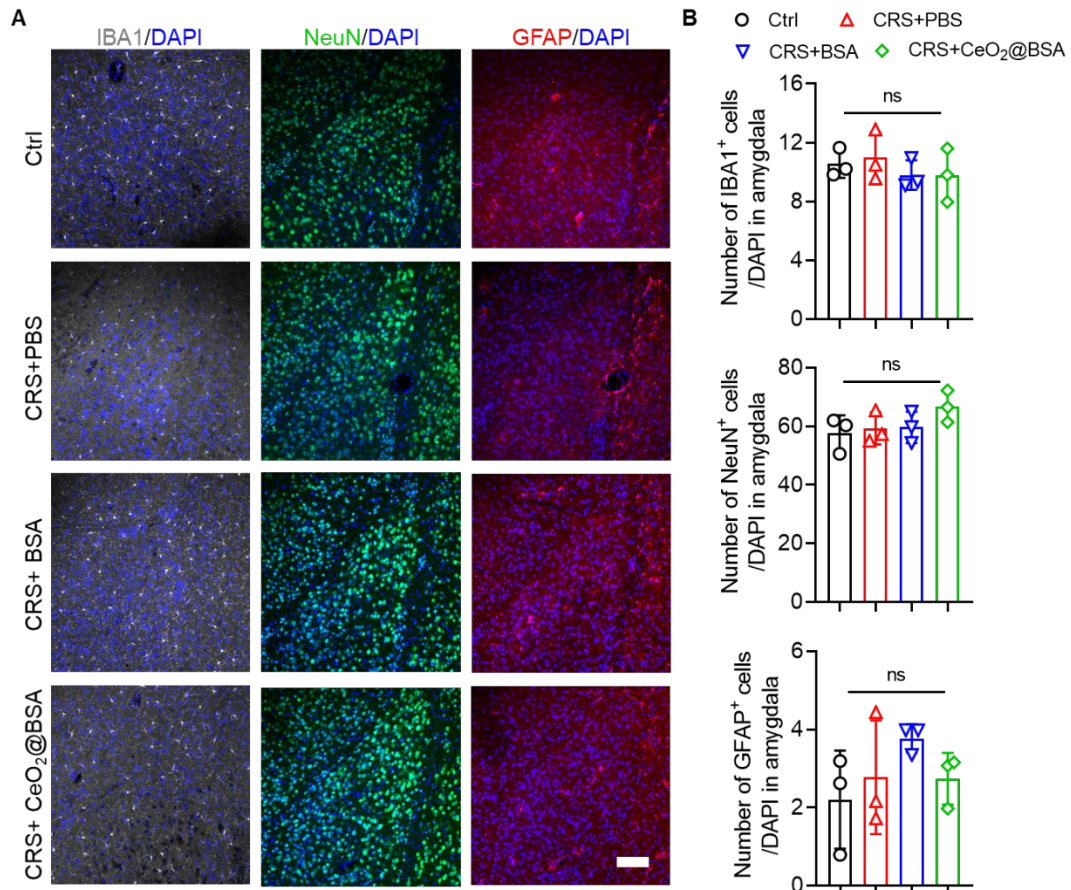
Supplementary Figure 4. Multiple ROS scavenging ability evaluation for CeO₂@BSA nanoclusters. (A) Superoxide anion scavenging ability evaluation for CeO₂@BSA nanoclusters. (B) Hydroxyl radical scavenging ability evaluation for CeO₂@BSA nanoclusters. (C) H₂O₂ scavenging ability evaluation for CeO₂@BSA nanoclusters.



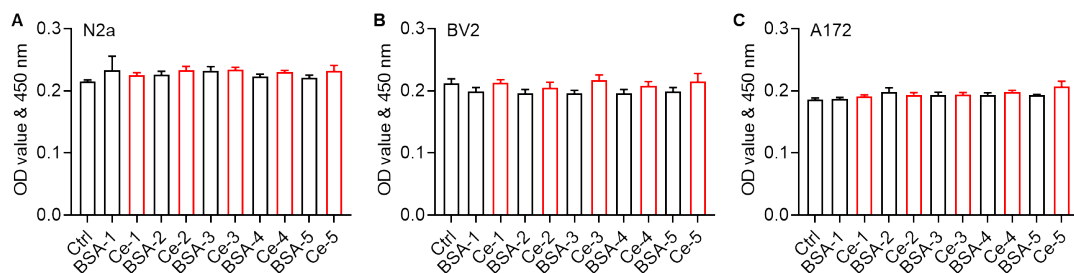
Supplementary Figure 5. Chronic restraint stress induces depressive behaviors and excessive ROS in brain. (A) Timeline of CRS model, depression-like behavior tests, and brain ROS detection. CRS model establishment: each mouse is restrained in a 50 mL respirable-centrifuge tube for 3 h every day last for 3 weeks. (B) Weight change of the mice before/after CRS versus that of control mice (n = 15). Depression-like behavior tests: (C) forced swimming test, (D) tail suspension test and (E) sucrose preference test (n = 15). (F) Open field test (n = 10). Flow cytometry detects for (G) negative, (H) control mice and (I) CRS mice brain total ROS. (J) A comparison of brain ROS level between control and CRS mice (n = 9). Data are shown as mean ± SD. Statistical analysis of (B) was performed by one-way ANOVA with a Tukey post hoc test and (C-F, J) was performed by unpaired Student's t-test, respectively.



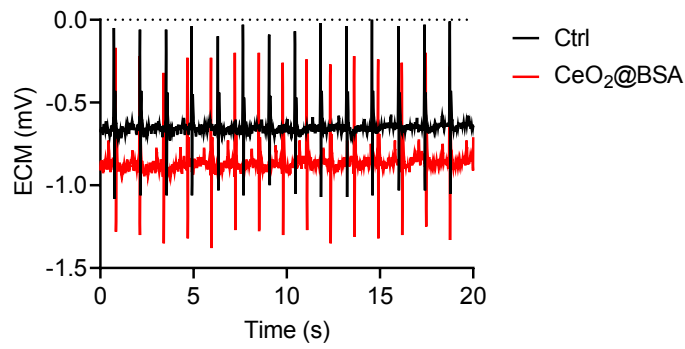
Supplementary Figure 6. (A) Immunofluorescent staining of hippocampus (Scale bar 100 μ m) and (B) quantitative results ($n = 3$). Data are shown as mean \pm SD. Statistical analysis was performed by one-way ANOVA with a Tukey post hoc test.



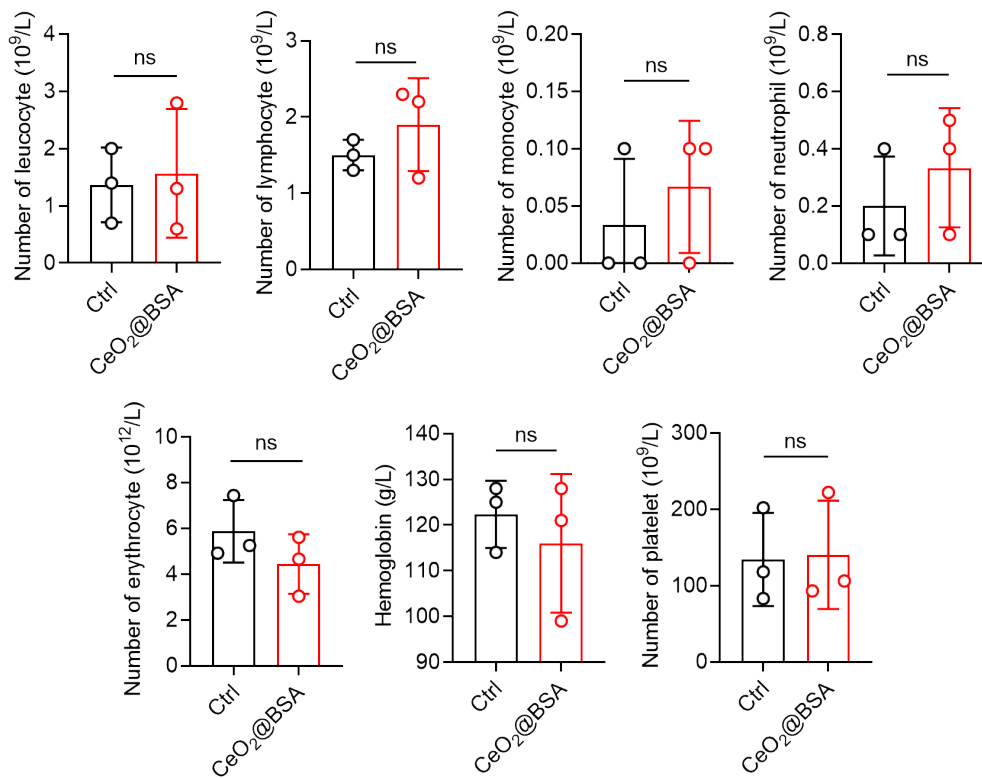
Supplementary Figure 7. (A) Immunofluorescent staining of amygdala (Scale bar 100 μm) and (B) quantitative results ($n = 3$). Data are shown as mean \pm SD. Statistical analysis was performed by one-way ANOVA with a Tukey post hoc test.



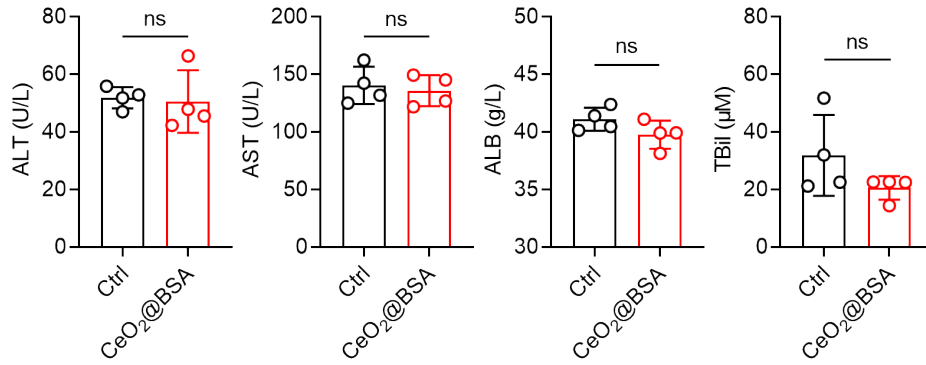
Supplementary Figure 8. Cell viability tests after CeO₂@BSA nanoclusters treatment for 24 h on (A) Neuro-2a (B) BV2 microglia and (C) A172 astrocyte. (The treating concentration was listed in Supplementary Table 2). Data are shown as mean \pm SD.



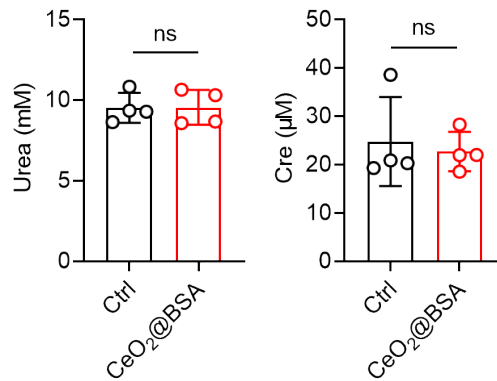
Supplementary Fig. 9. Electrocardiograph test for mice treatment with CeO₂@BSA nanoclusters and control.



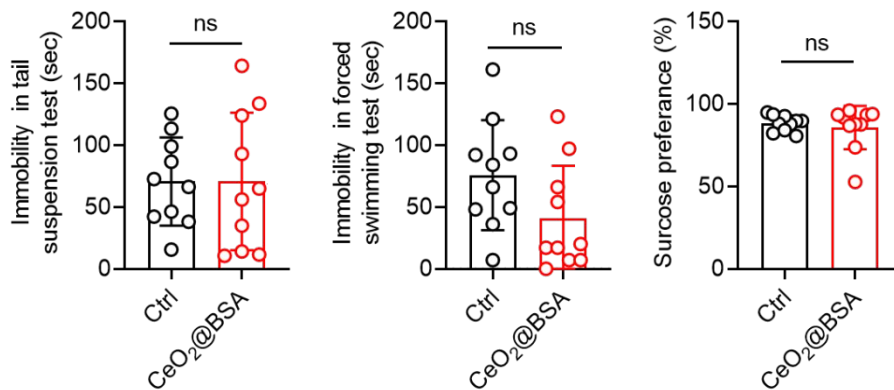
Supplementary Figure 10. Blood routine examinations for mice treatment with CeO₂@BSA nanoclusters and control (n = 3). Data are shown as mean ± SD. Statistical analysis was performed by unpaired Student's t-test.



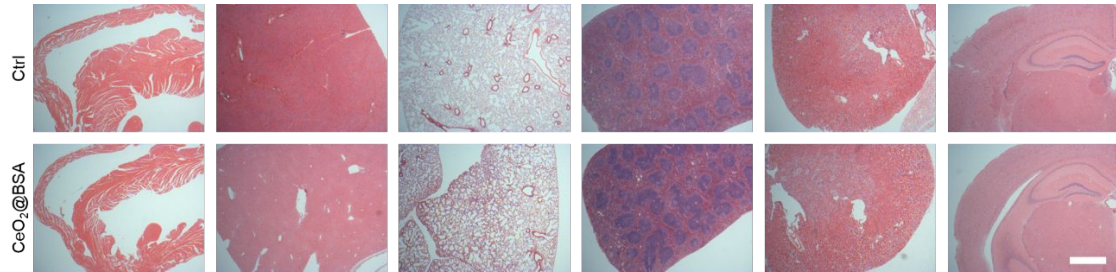
Supplementary Figure 11. Liver function tests for mice treatment with CeO₂@BSA nanoclusters and control (n = 4). Data are shown as mean ± SD. Statistical analysis was performed by unpaired Student's t-test.



Supplementary Figure 12. Kidney function tests for mice treatment with CeO₂@BSA nanoclusters and control (n = 4). Data are shown as mean ± SD. Statistical analysis was performed by unpaired Student's t-test.



Supplementary Figure 13. Depressive-like behaviors test for mice treatment with CeO₂@BSA nanoclusters and control (n = 10). Data are shown as mean ± SD. Statistical analysis was performed by unpaired Student's t-test.



Supplementary Figure 14. Representative H&E staining of mice main tissues post CeO₂@BSA nanoclusters intravenous injection (Scale bar 1 mm).

Supplementary Table 1. The different ratio of BSA to Ce³⁺ for CeO₂@BSA synthesis

Name	BSA (mg)	0.2 M Ce ³⁺ (μL)	Particle size (nm)
300Ce	25	300	140
250Ce	25	250	68
200Ce	25	200	21
150Ce	25	150	7.5
100Ce	25	100	6.4
50Ce	25	50	5.6
25Ce	25	25	4.8
10Ce	25	10	3.6

Supplementary Table 2. A comparison of the nanoceria with ROS scavenging ability.

Component	Average size (nm)	Superoxide anion scavenging ability (Ce ions concentration)	Hydroxyl radical scavenging ability	H ₂ O ₂ scavenging ability	Ref.
PEG modified CeO ₂	3	40% (0.4 mM)	Not mentioned	Not mentioned (Evaluated by O ₂ generation)	1
Triphenylphosphonium-conjugated CeO ₂	3	80% (1.5 mM)	Not mentioned	45% (1.5 mM)	2
RITC modified CeO ₂	3.3	80% (1.6 mM)	Not mentioned	75% (1.5 mM)	3
CeO ₂ @BSA	2	66% (0.145 mM)	16% (1.45 mM)	45% (1.45 mM)	

Supplementary Table 3. The concentration of CeO₂@BSA and BSA for cell viability tests.

Name	BSA (μg/mL)	Name	CeO ₂ @BSA (μg/mL)
BSA-1	12.5	Ce-1	12.5
BSA-2	25	Ce-2	25
BSA-3	50	Ce-3	50
BSA-4	100	Ce-4	100

Supplemental Materials and Methods

Mice. Male C57BL/6J mice (8-9 week) were housed and bred in the Comparative Medicine animal facilities of Tongji University School of Medicine. All procedures were conducted according to protocols approved by the Institutional Animal Care and Use Committee of Tongji University School of Medicine (reference number: SYXK (HU) 2014-0026).

Chronic restraint stress model. 50 mL centrifuge tubes were used for restraining device, with drilled holes (1 cm diameter) for mouse breath. Each mouse was restrained in the tube for 3 h once daily for 3 weeks.

Depression-related behavior tests. Forced swimming test (FST): Each mouse was forced to swim in a glass cylinder (height: 30 cm, diameter: 20 cm) filled with water (23–25 °C, 15 cm height) for 6 min. The immobility time in the final 4 min of each mouse was recorded. Tail suspension test (TST): Each mouse was suspended by the tail with its head 25 cm away from a table using adhesive tape for 6 min, and the immobility time in the final 4 min was recorded. Sucrose preference test (SPT): Each mouse was adapted to two bottles of water, two bottles of 2% sucrose solution, and water deprivation, respectively for 24 h. On test day, mouse was given one bottle of water and one bottle of sucrose solution. The 2 h consumption of two types of solution was weighed and the sucrose preference level was calculated.

Open field test. Each mouse was placed in an open field area (height: 40 cm, length: 40 cm, width: 40 cm) for free exploration for 6 min. The last 5 min distance of each mouse was recorded.

Brain ROS detection. Brain tissues were rapidly isolated after mice anesthesia for preparing cell suspension. Tissues were homogeneously minced and digested with 2.5% trypsin without phenol red and EDTA for 1 h. After passing 70 µm and 40 µm filters respectively, single-cell suspension was obtained. Then, catalyst and DCFH solution were added according to the protocol of the ROS assay kit (Abcam, # ab238535). After 30 min incubation and thrice rinses, the ROS signal was analyzed by flow cytometry (BD-LSRFortessa, BD).

Reagents. Bovine serum albumin (> 98%) and $\text{Ce}(\text{NO}_3)_3 \cdot 6\text{H}_2\text{O}$ (> 99%) were purchased from Sigma-Aldrich Trading Co., Ltd. (Shanghai, China). Sodium hydroxide (NaOH) was purchased from Sinopharm Chemical Reagent Co., Ltd. (Shanghai, China). Ultrapure water ($18.2 \text{ M}\Omega \text{ cm}^{-1}$) was purified by a Milli-Q system.

Synthesis of $\text{CeO}_2@$ BSA nanoclusters. $\text{CeO}_2@$ BSA nanocluster was synthesized by a biomimetic method. Typically, 125 mg BSA powders were dissolved in 50 mL deionized water at 37°C along with magnetic stirring, and 700 μL $\text{Ce}(\text{NO}_3)_3 \cdot 6\text{H}_2\text{O}$ solution (100 mM) was gradually added. Then, the solution pH was adjusted to 10-11 by NaOH. After 6 h reaction, $\text{CeO}_2@$ BSA nanocluster solution was dialyzed ($M_w = 10 \text{ kDa}$) against fresh ultrapure water for 24 h. The $\text{CeO}_2@$ BSA nanocluster powder was obtained via freeze drying.

Characterization of $\text{CeO}_2@$ BSA nanoclusters. TEM and high-resolution transmission electron microscopy (HRTEM) were conducted with a JEM-2100 microscope operated at 200 kV and a JEM-2100 microscope equipped with an EDX energy-dispersive spectrometer. Size and stabilization were evaluated by dynamic light scattering (DLS, Nano-ZS90, Malvern) and ultraviolet-visible (UV-vis) spectrophotometry (Nanodrop 2000, Thermo Fisher). TGA was conducted by Mettler Toledo TGA/DSC3+. The ion concentration was measured by inductively coupled plasma mass spectrometry (ICP-MS, iCAP RQ, Thermo Fisher). XPS was conducted on a PHI-5000C ESCA system (Perkin Elmer) with Mg $K\alpha$ radiation using an internal standard (C1s peak at 284.6 eV).

EPR spectrum was performed to determine the hydroxyl radical and superoxide anion scavenging ability of the $\text{CeO}_2@$ BSA nanoclusters. Hydroxyl radical was generated from UV-laser irradiated hydrogen peroxide, and was captured by BMPO. Superoxide anion was generated by the reaction between 2.5 mM KO_2 and 3.5 mM 18-crown-6, and was captured by DMPO. The magnetic field signals were detected by spectrometry (Bruker A300, Germany).

Cell culture. N2a, BV2 and A172 cells were used. N2a and BV2 cells were cultured in DMEM supplemented with 10% fetal bovine serum and 1% streptomycin and penicillin in a 37°C incubator. A172 cells were cultured in DMEM/F12 containing the same

concentrations of FBS and antibiotics.

ROS scavenging ability of CeO₂@BSA nanoclusters. In solution: superoxide anion, hydroxyl radical and hydrogen peroxide scavenging capacities of the CeO₂@BSA nanoclusters were determined by assay kits (Jiancheng, Nanjing). Superoxide anion generated by the reaction between xanthine and xanthine oxidase, and hydroxyl radical produced by the Fenton reaction were both determined at a wavelength of 550 nm via chromogenic Griess reagent. Hydrogen peroxide were detected by ammonium molybdate to form a yellow solution with an absorbance peak at 405 nm.

In vitro: a ROS assay kit consisting of a DCFH-DA probe and Rosup (a positive control) was employed to evaluate the in vitro ROS-scavenging capacity of CeO₂@BSA. N2a, BV2 and A172 cells were seeded in 24-well plates, and Rosup-treatment induced a high ROS model. The medium was replaced with CeO₂@BSA nanoclusters or BSA solution for 2 h. Afterwards, the cells were washed with serum-free medium thrice, and fresh medium containing 10 μM DCFH-DA probe was added for 30 min. Finally, the cells were washed thrice with serum-free medium for fluorescence imaging.

Pharmacokinetics and biodistribution of CeO₂@BSA nanoclusters. The pharmacokinetics of CeO₂@BSA nanoclusters was assessed by measuring the Ce ion concentration in mouse blood. 300 μL CeO₂@BSA nanoclusters were intravenously administrated into mice tail vein, and the 5 μL fresh blood was squeezed at different time point for ICP-MS.

The biodistribution of the CeO₂@BSA nanoclusters was assessed by measuring the Ce ion concentration in mouse main tissues. 300 μL CeO₂@BSA nanoclusters were intravenously administrated into mice tail vein, and mice were sacrificed post 30 min. To avoid blood interference, mice were perfused with PBS and major tissues (heart, liver, spleen, lung, kidney and brain tissues) were isolated for ICP-MS. The brain accumulation of Ce ion concentration at different time point post administration was similarly measured.

To assess metabolism, the feces and urine of CeO₂@BSA nanoclusters treated mice were collected at different time points (8 h, 24 h, 48 h and 72 h), for Ce ion measurement by ICP-MS.

For fluorescence imaging, Cy5-NHS was used to label the amino of CeO₂@BSA. 300 µL Cy5-labeled CeO₂@BSA nanoclusters were intravenously administrated into mice tail vein, and the whole body of mice was recorded at different time points by an in vivo fluorescence imaging system (VISQUE Invivo Smart-LF, Vieworks). The brain tissue was isolated from the perfused mice at different time point for fluorescence imaging. For immunohistochemical staining, mice brain slices (30 µm) were obtained by freezing microtome, and fixed in 4% paraformaldehyde overnight with 3 times PBS wash. The brain slices were blocked in 3%BSA, 10% goat serum and 1% Triton X100 (Bio-Rad) in PBS for 1 h, then incubated with the primary antibodies (MAP2, mouse, cat# MB0078, Bioworld, 1:100; IBA1, goat, cat# ab5076, Abcam, 1:100; GFAP, chicken, cat# AB5541, Millipore, 1:500) overnight at 4°C. Next, brain slices were washed with PBS and incubated with secondary antibodies for imaging (FV3000, Olympus).

Immunofluorescent staining. Brain sections were fixed in 4% paraformaldehyde and washed three times with PBS. Brain sections were incubated in permeabilization and blocking buffer (3% BSA, 10% donkey serum, and 1% Triton X-100 in PBS) for 1 h at room temperature. Then the sections were incubated with primary antibodies including IBA1 (Abcam, cat #ab5076, goat, 1:200), NeuN (Cell signaling technology, cat #12943, rabbit, 1: 400), GFAP (Sigma, cat #AB5541, chicken, 1:400), BDNF (Abcam, cat #108319, rabbit,1:500) overnight at 4 °C. Then, all sections were washed with PBS and incubated with secondary antibody and DAPI for 1 h. Immunofluorescence was observed under a confocal microscopy (FV3000, Olympus).

Western blotting. Protein was extracted from the brain tissues using Protein Extraction Buffer (Pierce) containing protease inhibitor cocktail (Sigma), and the protein concentration was determined by BCA method. Next, the proteins were separated by SDS-PAGE and electrophoretically transferred on to polyvinylidene fluoride membranes (Millipore and Bio-Rad). The membranes were incubated with primary antibodies PSD95 (Cell signaling technology, cat #3450s, rabbit, 1: 1000), synaptophysin (Synaptic system, cat #101002, rabbit, 1: 1000), BDNF (Abcam, cat #ab108319, rabbit, 1:1000) and β-actin (mouse, cat# a5441, Sigma, 1:5000) against

overnight at 4 °C, and then incubated with a horseradish peroxidase-linked anti-rabbit or anti-mouse secondary antibody (Cell Signaling Technologies, 1:5000). The bands were visualized with Pierce ECL Western Blotting Substrate (Thermo Fisher Scientific, Waltham, MA, United States).

Biocompatibility evaluation of CeO₂@BSA nanocluster. *In vitro*: The biocompatibility was determined by the CCK-8 assay. N2a, BV2 and A172 cells were respectively seeded in 96-well plates at a density of 10⁴ cells per well at 37 °C and 5% CO₂ incubation environment. After 24 h, the medium was removed and replaced with fresh culture medium containing different concentrations of CeO₂@BSA nanocluster/BSA (Supplementary Table 1). After 1 day incubation, the culture medium was replaced with CCK-8 solution (10 μL/100 μL medium) for 30 min incubation. Then, cell viability was measured by the absorbance at 450 nm with a microplate reader (Versa Max, Molecular Devices).

In vivo: Mice were intravenously treated with 300 μL CeO₂@BSA nanocluster every other day last for 6 days. ECG was conducted to evaluate mouse heart function (Labchart, ADInstruments). Mice blood were collected for blood panel analysis and serum biochemistry tests for alanine aminotransferase (ALT), aspartate aminotransferase (AST), ALB, TBil, urea and Cre levels. The presence of occult blood and transferrin in excreted feces was assessed with test strips. Depression- and anxiety-like behaviors were assessed by the TST, FST and SPT. Major tissues, including heart, liver, spleen, lung, kidney and brain tissues, were isolated for H&E staining.

Statistical analyses. Differences between two independent groups was analyzed by unpaired Student's *t*-test, and for multiple group the comparison was analyzed by one-way ANOVA with Tukey post-correction. Data were shown as mean ± SD, and significance was determined as *p* < 0.05.

References:

1. Weng, Q.; Sun, H.; Fang, C.; Xia, F.; Liao, H.; Lee, J.; Wang, J.; Xie, A.; Ren, J.; Guo, X.; Li, F.; Yang, B.; Ling, D. Catalytic activity tunable ceria nanoparticles prevent chemotherapy-induced acute kidney injury without interference with chemotherapeutics, *Nat Commun* **2021**, 12, (1), 1436.

2. Kwon, H. J.; Cha, M. Y.; Kim, D.; Kim, D. K.; Soh, M.; Shin, K.; Hyeon, T.; Mook-Jung, I. Mitochondria-Targeting Ceria Nanoparticles as Antioxidants for Alzheimer's Disease, *ACS Nano* **2016**, 10, (2), 2860-70.
3. Kim, C. K.; Kim, T.; Choi, I. Y.; Soh, M.; Kim, D.; Kim, Y. J.; Jang, H.; Yang, H. S.; Kim, J. Y.; Park, H. K.; Park, S. P.; Park, S.; Yu, T.; Yoon, B. W.; Lee, S. H.; Hyeon, T. Ceria nanoparticles that can protect against ischemic stroke, *Angew Chem Int Ed Engl* **2012**, 51, (44), 11039-43.